PROCEEDINGS OF ECOS 2023 - THE 36TH INTERNATIONAL CONFERENCE ON
EFFICIENCY, COST, OPTIMIZATION, SIMULATION AND ENVIRONMENTAL IMPACT OF ENERGY SYSTEMS
25-30 JUNE 2023, LAS PALMAS DE GRAN CANARIA, SPAIN

Hierarchical Distributed Model Predictive Control for Building Energy Systems

Maximilian Mork[a], André Xhonneux[b] and Dirk Müller[c,d]

[a] Forschungszentrum Jülich, Institute of Energy and Climate Research, Energy Systems Engineering (IEK-10), Jülich, Germany, m.mork@fz-juelich.de, CA
[b] Forschungszentrum Jülich, Institute of Energy and Climate Research, Energy Systems Engineering (IEK-10), Jülich, Germany, a.xhonneux@fz-juelich.de
[c] Forschungszentrum Jülich, Institute of Energy and Climate Research, Energy Systems Engineering (IEK-10), Jülich, Germany, di.mueller@fz-juelich.de
[d] RWTH Aachen University, E.ON Energy Research Center, Institute for Energy Efficient Buildings and Indoor Climate, Aachen, Germany, dmueller@eonerc.rwth-aachen.de

Abstract:
Buildings contribute to approximately 30 % of global energy consumption, which renders their energy-efficient control an effective measure to reduce overall energy consumption. This paper presents a hierarchical distributed Model Predictive Control (MPC) for building energy systems based on nonlinear Modelica controller models. It combines hierarchical and distributed optimization approaches to split the optimization complexity within the temporal and spatial dimension. The hierarchical optimization approach considers different dynamics in complex building energy systems and ensures both anticipation for systems with high inertia and reactivity with regard to errors in the forecasting of the disturbance quantities. The distributed optimization approach divides the centralized optimization problem into subproblems to improve the scalability and adaptability of the control framework. The subproblems are solved in a parallel and iterative manner and account for both thermal (heat transfer over zone boundaries) and hydraulic inter-zone coupling (induced by a central, shared Heating, Ventilation and Air Conditioning (HVAC) system). A particular focus of the control approach is placed on robustness with respect to errors in the forecasting of the disturbances that impact the building dynamics. The control performance of the proposed MPC framework is evaluated in a simulative case study of heating and shading control of a nonlinear six-room-building Modelica model, which is exposed to different forecast accuracies for the disturbances of occupancy, solar radiation and air exchange. The case study exhibits the benefits of the control framework in terms of energy consumption, thermal discomfort and computation time in comparison to a reference control concept of a non-hierarchical distributed MPC configuration.

Keywords:
Distributed MPC; Hierarchical MPC; HVAC; Model Predictive Control (MPC); Modelica.

1. Introduction

Approximately 30 % of global energy consumption and 27 % of CO_2 emissions are attributed to the building sector [1]. Heating, Ventilation and Air Conditioning (HVAC) systems contribute to a major extent to building energy consumption [2] and therefore, offer a large potential for an increase in energy efficiency and reduction of energy consumption on a global scale. Currently, conventional control strategies as Rule-Based Control (RBC) or Proportional-Integrative-Differential (PID) controllers are implemented in buildings due to their simplicity and low computational requirements [3]. They represent inflexible and reactive (non-predictive) control approaches that are unable to control inert systems with large time delays, to minimize energy consumption while operating between comfort bounds as well as to consider system or comfort constraints and future disturbances.

Model Predictive Control (MPC) constitutes a promising control approach that addresses the aforementioned challenges and exhibits various benefits and energy savings from 15 to 50 % [4] compared to the conventional control strategies. The central part of an MPC is a model of the building energy system based on which future system behavior is predicted and the building is controlled in an anticipatory manner minimizing a (multi-objective) cost function over a prediction horizon. The predictive characteristic of the control suits inert systems with time delays and integrates future disturbances, e.g., in the form of weather and occupancy forecasts. Apart from this, conflicting optimization goals such as the simultaneous minimization of discomfort and energy consumption as well as system and comfort constraints can be taken into account.

The model generation part is crucial for the implementation of an MPC as it consumes most of the project time and costs [5]. Due to the unique characteristics of every single building, a modeling language has to

https://doi.org/10.52202/069564-0220

be modular and flexible and support the user-friendly generation of (large-scale) building models. The modeling language Modelica [6] complies with these requirements as it supports open-source, equation-based, acausal and object-oriented modeling and is equipped with a user-friendly graphical interface for connecting and parametrizing components. Modelica allows for the collection of building component models in shareable libraries such as the Modelica IBPSA library [7] or extensions building upon this library.

If MPC is applied to large-scale multi-zone buildings, large and computationally complex optimization problems are created, which results in increased computation times. This can also lead to scalability issues when the optimization problems cannot be solved in a suitable time restricting the real-time capability of the control. Distributed MPC approaches tackle these challenges by splitting the central optimization problem into subproblems, which are solved in a distributed manner while accounting for the interactions between the subproblems [8].

On the other hand, buildings generally incorporate components and disturbances of different dynamics and time scales. For example, low-temperature heating and cooling systems based on Thermal Activated Building Systems (TABS) are characterized by a high thermal mass and large time constants requiring a long prediction horizon. They are often complemented by secondary, more reactive actuators such as radiators or convectors, where smaller prediction horizons and control periods are suitable. The simultaneous control of actuators of different time scales and preservation of both anticipation and reactivity poses an additional challenge for the application of MPC in buildings. An approach to tackle this challenge is hierarchical MPC, which splits the optimization problem into layers of different dynamics [8].

Compared to the total number of studies on building MPC, the review of literature for MPC in large-scale buildings exhibits only a relatively small share of distributed optimization approaches. This may be attributed to the nonlinear and nonconvex characteristics of building energy systems that complicate convergence of the distributed optimization approaches [4]. The most widely applied mathematical methods for distributed building MPC are the primal-dual active-set method [9], Benders decomposition [10], dual decomposition [11], information exchange [12], non-iterative look-up tables [13], Nash equilibrium [14, 15] or Alternating Direction Method of Multipliers (ADMM) [16–19]. Among these, Nash equilibrium constitutes an uncooperative, parallel and iterative distributed optimization approach, which builds upon information exchange between subsystems. After every iteration, each subsystem sends and receives updated trajectories for the coupling variables to/from interconnected subsystems and solves its subproblem again. The subsystems converge to a ”Nash equilibrium” if for all subsystems, the local optimization results deviate less than a predefined threshold between two consecutive iterations. Nash equilibrium is applied for considering thermal coupling based on exchanged local temperature trajectories [14] or for taking into account hydraulic control input coupling [15]. ADMM represents a distributed optimization approach with an iterative and cooperative structure, which is carried out mostly in parallel. It is based on the augmented Lagrangian, i.e., the Lagrangian formulation plus an additional quadratic penalty term for improved convergence and robustness compared to dual decomposition. ADMM makes use of two sets of variables, which allows separating the central cost function and coupled dynamics as well as splitting the problem into subproblems. The fulfillment of the coupling constraints between the different variable sets is steered via dual variables penalizing the deviations within the cost functions. ADMM is applied for considering thermal and hydraulic coupling [16], indoor air quality in rooms coupled by a central Air Handling Unit (AHU) [17], maximum constraints on shared resources (e.g., maximum capacity of an AHU) [18] and sharing problems (sum of local control variables is input to the global cost function) [19].

Hierarchical building MPC approaches are applied to split optimization problems into different layers with varying dynamics and time scales, which are controlled based on different prediction horizons and sampling periods. Abreu et al. [20] implement a hierarchical building MPC, which consists of a scheduling layer sending output trajectories and power profiles to the lower layer with a shorter prediction horizon and sampling period. The latter tracks the forwarded output trajectories while taking into account the constraining trajectory of the power profile. Fiorentini et al. [21] implement a hierarchical MPC for the operation of an HVAC system including an AHU coupled to a thermal storage. The upper layer with a longer prediction horizon and sampling period calculates an optimal sequence of discrete operating modes, which are executed by the lower level while tracking a reference temperature sent by the upper level. Long et al. [22] develop a distributed hierarchical MPC controlling a ventilated multi-zone building. An upper centralized layer calculates reference temperature trajectories for a lower layer consisting of several local controllers, which solve their local problems in an isolated, decentralized way based on local information and the upper temperature trajectories to be tracked.

In previous works, the concepts of hierarchical [23] and distributed [24] building MPC based on nonlinear Modelica models have been individually developed. The hierarchical MPC splits the optimization problem into two layers of different dynamics, which are equipped with different prediction horizons and sampling periods to guarantee both anticipation and reactivity. The distributed MPC splits the centralized optimization problem into subproblems and takes into account thermal and hydraulic coupling between building zones using an optimization approach based on Nash equilibrium and ADMM. In this work, the hierarchical and distributed

https://doi.org/10.52202/069564-0220

MPC approach are combined into one MPC framework and applied to a multi-zone building that incorporates actuators of different dynamics. The control quality and the reactivity of the MPC are evaluated for different scenarios of forecasting accuracy for the disturbance quantities. The forecast errors can be regarded as any deviation between the predicted and actual real-world behavior of the building, which are expected to appear in practical MPC implementations. By using the hierarchical distributed MPC approach, the complexity of the original optimization problem is split in both the temporal and spatial dimension. This alleviates modular, local high-accuracy modeling and at the same time, improves the scalability, real-time capability and adaptability of the control approach.

2. Methodology

2.1. Distributed MPC

The methodology for the distributed MPC has been elaborated in [24]. The approach considers both thermal and hydraulic coupling among different building zones and is executed in an iterative and parallel way. It is based on an uncooperative optimization approach for thermal coupling using Nash equilibrium and a cooperative approach for hydraulic coupling using ADMM. A central coordinator updates information and monitors the convergence process of the overall optimization.

The uncooperative Nash optimization regards the room temperatures of neighboring zones as known disturbances and thereby, can calculate the heating flows exchanged over the local zone boundaries. After every optimization iteration, the locally calculated trajectories for the local room temperatures are sent to the coordinator. The coordinator forwards the temperature trajectories to all neighboring zones that are thermally coupled to the corresponding zone and the local optimizations are executed again with updated trajectories for the neighboring room temperatures. The local subproblems converge to the ”Nash equilibrium” if, for all local subsystems, averaged over the MPC horizon, the absolute deviation of the local room temperature trajectories between two consecutive distributed iterations does not deviate more than a prefixed Nash threshold.

The hydraulic coupling comprises interactions between the zones induced by a shared, central HVAC system. In the case study in Section 3., the central HVAC system is constituted by a shared TABS in the form of Concrete Core Activation (CCA) in the floor. TABS builds upon the activation of the thermal mass of a building in the form of the concrete and offers passive storage capacities to shift the time between energy supply and demand. Due to the high inertia of the thermal mass, one TABS/CCA section generally supplies multiple building zones with similar thermal properties, demand or orientation [25], which introduces strong coupling between the rooms. Within the case study, the central CCA consists of six identically dimensioned subsections (one per room) and is controlled via one shared control input that regulates the supply water mass flow supplied to each subsection. The hydraulic coupling is taken into account using a consensus ADMM approach. The optimization problem is decomposed by introducing local copies of the global CCA control input for every subsystem, which are optimized separately. Linear and quadratic ADMM terms are added to the cost functions of both the local subsystems (1) and the coordinator (2) to coordinate the consistency between the local copies and the global CCA control input. The coordinator monitors the convergence of the ADMM applying both a primal and dual residual criterion according to [24, 26].

The communication structure of the overall distributed optimization approach is shown in Fig. 1. In every distributed optimization iteration, the local subproblems (1) are optimized in parallel and the resulting local trajectories for the CCA control input and room temperature are sent to the global coordinator. The global coordinator uses the updated information to optimize the global cost function calculating new trajectories for the global CCA control input (2). In the second step, the dual ADMM variables (Lagrangian multipliers) are updated coordinating the consistency between the global and local copies of the CCA control input (3). The coordinator checks the convergence status for both ADMM and Nash optimization according to the user-specified thresholds. Then it forwards the trajectories for the global CCA control input, dual variables, local room temperatures and the convergence status to the subproblems, which continue the local optimization procedures according to the convergence status. If the subproblems have converged, they send the local control inputs for all actuators to the global coordinator, which converts the local CCA control inputs into an averaged value and runs a simulation over a sampling period (right branch). If the subproblems have not converged and the maximum number of distributed iterations per MPC iteration is not exceeded, the subproblems are solved again based on the new information sent by the global coordinator (left branch).

2.2. Hierarchical MPC

The hierarchical MPC divides the optimized problem within the temporal dimension into two layers of different dynamics and time scales as proposed in [23]. For the upper, slow MPC layer, a longer prediction horizon and sampling period are chosen, whereas for the lower, fast layer, the horizon and sampling period are smaller. Thereby, the slow layer focuses on anticipation of the control, which is specifically suitable for inert systems with time delay (e.g., TABS or thermal storage). Due to the small sampling periods of the fast MPC layer,

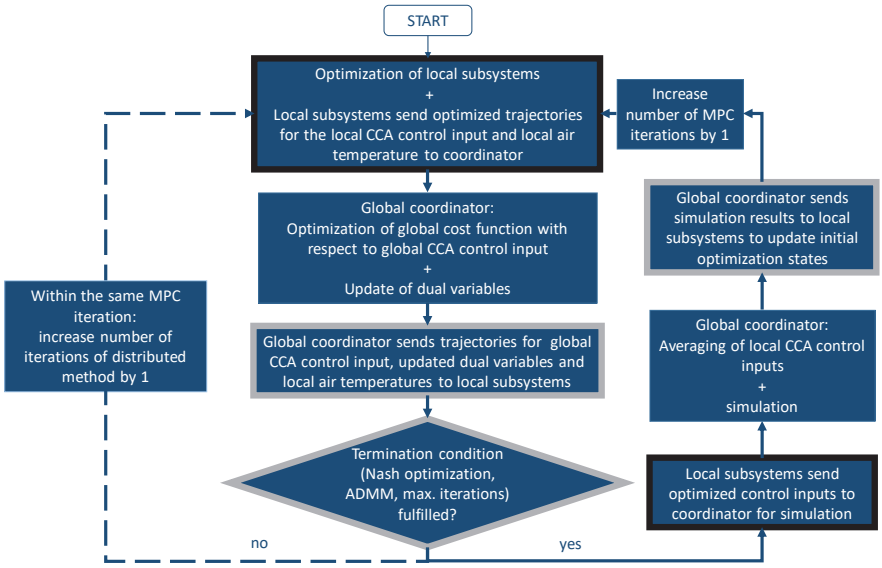

Figure 1: Overall communication structure of the distributed MPC (inputs to local MPC: gray frame, outputs of the local MPCs: black frame)

reactivity with regard to forecasting or unexpected influences can be ensured. The two layers communicate via state reference trajectories that are calculated by the slow layer and are sent to the fast layer to be tracked. Compared to a single MPC layer equipped with a long prediction horizon and small sampling period, the combination of the two layers increases the probability to preserve real-time capability.

2.3. Hierarchical Distributed MPC

The scheme of the aggregated hierarchical distributed MPC toolchain for the six-room-building use case is depicted in Fig. 2. Both the upper and lower hierarchical MPC layer are split into thermal zone subproblems in a distributed way (for each of the six rooms). Within each MPC layer, the subproblems are solved based on the distributed optimization approach based on Nash equilibrium and ADMM. An overall distributed MPC iteration is terminated if, in both the upper and lower MPC layer, the convergence criteria for the Nash equilibrium and ADMM are fulfilled or the maximum number of distributed iterations in one MPC iteration is exceeded. The cost functions of the subproblems in the lower layer contain quadratic tracking terms for the room temperature trajectories $T_{\mathrm{ref,i}}$ calculated by the room equivalent on the upper layer. The reference trajectories are recalculated in every distributed iteration of the upper MPC layer and the updated trajectories are forwarded to the lower layer. After convergence, the control inputs of the lower MPC layer are applied to the simulation model and based on the simulation results, the optimization states of the next optimization iteration are initialized both in the upper and lower MPC layer.

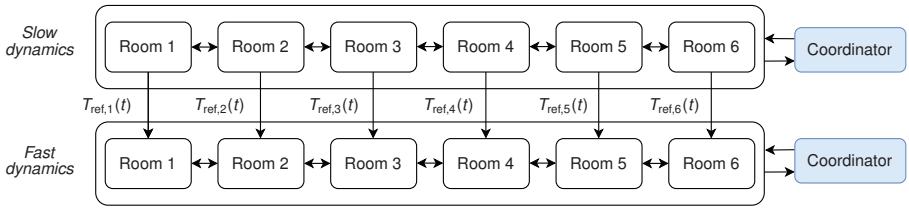

Figure 2: Communication structure of the hierarchical distributed MPC

3. Case study

In a simulative use case, the hierarchical distributed MPC is applied to the six-room-building shown in Fig. 3. The nonlinear model is generated based on the Modelica building simulation library AixLib [27] and comprises rooms that are thermally coupled via inner walls and data-driven models for air flow through doors [24]. All rooms are hydraulically coupled to a central, shared TABS implemented as CCA in the floor, which is operated via a central control input regulating the supply water mass flow. Each room is equipped with an identically

https://doi.org/10.52202/069564-0220

dimensioned CCA subsection, a convector, simplified pumps and an external window including external Venetian blinds for active solar shading [23]. Two pumps per room supply the CCA subsection and the hydraulically uncoupled convector with supply water mass flow rates calculated by the optimization (at fixed supply temperatures).

Control inputs of the subsystems are the local water mass flow rates to the convectors and the vertical position and inclination angle of the Venetian blinds. The shared control input of the central mass flow rate to the CCA applies to all subsystems. For occupant comfort, both thermal and visual comfort (minimum illuminance of 500 lux in occupied times) are considered. During the occupied periods (8 a.m.–12 p.m. and 1–6 p.m.), there is one person in rooms 3 and 5, two persons in rooms 1 and 6 and three persons in rooms 2 and 4. During unoccupied times the thermal comfort ranges are broadened according to a night set-back (occupied times: 293–295.5 K, unoccupied times: 292–296.5 K). Weather data is integrated based on an AixLib resource file of San Francisco, which represents a heating period. No model mismatch between the MPC controller and the simulation model is assumed to focus on the control performance of the hierarchical distributed MPC.

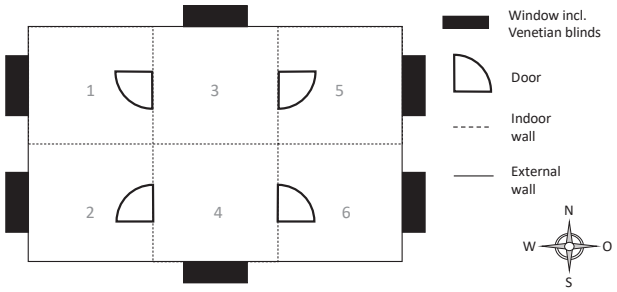

Figure 3: Building structure consisting of six thermal zones

For every subsystem $i \in \mathcal{N}$, the following local optimization problem is solved (for distributed iteration $k + 1$, the last term of the cost function including $T_{\text{ref,i}}$ is omitted for the upper hierarchical layer):

$$\{u_{\text{conv},i}, u_{\text{CCA,local},i}, u_{\text{al},i}, u_{\text{posShad},i}, u_{\text{inclAng},i}, \underline{\varepsilon}_i, \bar{\varepsilon}_i\}^{k+1} = \textit{argmin}_{u_{\text{conv},i}, u_{\text{CCA,local},i}, u_{\text{al},i}, u_{\text{posShad},i}, u_{\text{inclAng},i}, \underline{\varepsilon}_i, \bar{\varepsilon}_i}$$
$$\int_{t_0}^{t_f} [\alpha_{\text{conv}} \cdot u_{\text{conv},i} \cdot (T_{\text{supply,conv},i} - T_{\text{return,conv},i}) + \alpha_{\text{CCA}} \cdot u_{\text{CCA,local},i} \cdot (T_{\text{supply,CCA},i} - T_{\text{return,CCA},i}) +$$
$$\alpha_{\text{Light}} \cdot u_{\text{al},i} + \theta \cdot (\underline{\varepsilon}_i{}^2 + \bar{\varepsilon}_i^2) + \lambda^k_{\text{Dual,CCA},i} \cdot (u_{\text{CCA,local},i} - u^k_{\text{CCA,global}}) + \rho/2 \cdot (u_{\text{CCA,local},i} - u^k_{\text{CCA,global}})^2 +$$
$$\gamma \cdot (T_{\text{room,air,i}} - T_{\text{ref,i}})^2] \, dt \tag{1}$$

The local cost functions (1) consist of the energy consumption of the convector, CCA and artificial lighting as well as discomfort (quadratic penalization of temperatures outside the comfort range through introduced slack variables $\underline{\varepsilon}_i$ and $\bar{\varepsilon}_i$). The terms are complemented by the linear and quadratic ADMM terms taking into account the consensus between the local and global CCA control variables (based on the Lagrangian multipliers $\lambda^k_{\text{Dual,CCA},i}$ and the ADMM penalty parameter ρ). The last term in the cost function applies only to subsystems in the lower hierarchical MPC layer and comprises the quadratic tracking of the reference temperature trajectories $T_{\text{ref,i}}$ sent by the room equivalent on the upper layer (weighted with γ).

$u_{\text{conv},i}$, $u_{\text{CCA,local},i}$, $u_{\text{al},i}$, $u_{\text{posShad},i}$ and $u_{\text{inclAng},i}$ correspond to the local control inputs of the convector and CCA supply water mass flows, artificial lighting, shading position and inclination angle of the Venetian blinds. $T_{\text{room,air},i}$ is the local room air temperature. $T_{\text{supply,conv},i}$, $T_{\text{return,conv},i}$, $T_{\text{supply,CCA},i}$ and $T_{\text{return,CCA},i}$ are the supply and return water temperatures of the convector and CCA. α_{conv} and α_{CCA} are energy weighting factors for the convector and CCA including the heat capacity of water, α_{Light} a weighting factor for the energy consumption of artificial lighting and θ a factor penalizing room temperatures outside the comfort range. The prediction horizon (t_0 - t_f) is 24 h for the upper MPC layer and 8 h for the lower layer, the sampling period is set to 15 min for the upper and to 5 min for the lower layer.

Based on the calculated trajectories for the local room-individual CCA control inputs $u^{k+1}_{\text{CCA,local},i}$ from (1), the global coordinator calculates the global CCA control input $u_{\text{CCA,global}}{}^{k+1}$ for iteration $k + 1$ (2). In the second step, the dual variables (Lagrangian multipliers) $\lambda^{k+1}_{\text{Dual,CCA},i}$ are updated for every zone (3).

$$u_{\text{CCA,global}}{}^{k+1} = argmin_{u_{\text{CCA,global}}} \int_{t_0}^{t_f} [\sum_{i \in \mathcal{N}} \lambda^{k}_{\text{Dual,CCA},i} \cdot (u^{k+1}_{\text{CCA,local},i} - u_{\text{CCA,global}}) + \rho/2 \cdot (u^{k+1}_{\text{CCA,local},i} - u_{\text{CCA,global}})^2] dt \quad (2)$$

$$\lambda^{k+1}_{\text{Dual,CCA},i} = \lambda^{k}_{\text{Dual,CCA},i} + \rho \cdot (u^{k+1}_{\text{CCA,local},i} - u^{k+1}_{\text{CCA,global}}) \quad (3)$$

The control quality of the implemented hierarchical distributed MPC is evaluated in terms of the following Key Performance Indicators (KPIs): energy consumption (for CCA, convector and artificial lighting; in MJ), thermal discomfort (quantification of room temperatures outside the comfort range; in Kh) as well as total computation time and computational time ratio. The computational time ratio represents the ratio of the total computation time to the simulated control time. A quotient smaller than 1 is equivalent to real-time capability of the control. The performance of the proposed hierarchical distributed MPC is compared to a non-hierarchical distributed equivalent consisting of only one MPC layer with a prediction horizon of 24 h and a sampling period of 15 min.

The control quality of the different control approaches is evaluated for different accuracy scenarios for the disturbance forecasts. In the first scenario, a perfect forecast for the disturbance quantities of occupancy, solar radiation (global horizontal, diffuse horizontal and direct normal) and air exchange rate is assumed. For the second and third scenario, forecast errors are artificially generated according to a normal (Gaussian) distribution, zero mean and varied standard deviations σ (based on the Python package *numpy*). A filter extracts negative values for radiation and occupancy. The occupancy value is rounded to an integer and during unoccupied times, no forecast errors are added to occupancy and solar radiation. The forecast error for occupancy represents a higher/lower number of occupants than forecasted, the error for solar radiation expresses the occurrence of unexpected clouds and the error for the air exchange constitutes higher or lower wind speeds than forecasted, which impact the air exchange of the building with ambient air. In the simulative case study, an old building structure with loose air tightness and high air infiltration with a base air exchange of 2.5 1/h is assumed to generate substantial heat demand and transfer the heat from solar and internal gains. The forecast errors can be considered representative of any deviation between the predicted and the real-world behavior of the buildings, such as errors in weather or occupancy forecasts, model errors or unexpected user influences (e.g., window/door opening or manual heating/shading). The standard deviations determining the dimension of the forecast errors are increased in intervals of 0.5 for occupancy, in intervals of 50 W/m^2 for solar radiation and in intervals of 0.1 1/h for the air exchange. The standard deviations are noted in the following manner: $\sigma = (\sigma_{\text{occupancy}}[-], \sigma_{\text{radiation}}[W/m^2], \sigma_{\text{air exchange}}[1/h])$. The optimizations are executed in JModelica.org 2.14 [28] (using linear HSL solver ma27 [29]) for gradient-based optimization of Modelica models with an interface to IPOPT 3.13.1 [30]. The simulation on the coupled building model has a horizon of 5 days. The optimizations are executed on an OpenStack instance with Ubuntu 18.04, 8 vCPUs and 32 GB RAM.

4. Results

Forecast scenario σ = (0,0,0)

For the perfect forecast scenario, the disturbances of outdoor temperature, solar radiation on each window facade and occupancy are depicted in Fig. 4. The results of the non-hierarchical and the hierarchical distributed MPC are shown in Fig. 5 and Fig. 6. The three last subplots ”Actuator mass flow”, ”Shading position” and ”Inclination angle” reveal a more dynamic operation of the control inputs for the hierarchical variant compared to its non-hierarchical equivalent, which is due to the higher temporal resolution and reactivity of the lower layer of the hierarchical MPC. At intervals of 5 min (compared to 15 min for the non-hierarchical variant), the hierarchical MPC receives updated measurements from the building and readjusts the control inputs. Since for the first scenario a perfect forecast is assumed, the local room temperatures in the ”Local temperature” subplots resemble each other apart from individual violations at the beginning and end of the simulation horizon. The CCA covers the base load benefiting from a higher energy efficiency due to lower supply temperatures and is preheated to cover the heat demand at a later time, while the convectors are operated in a more reactive manner to cover peak loads. During the periods with heat gains from occupancy and solar radiation, the rooms are operated near the upper temperature bound to reduce heating and lighting energy by actively using the Venetian blinds to limit solar gains. During the non-occupancy periods, the temperatures are kept near the lower bound taking advantage of the night set-back to decrease heating energy consumption. The consumed energy is of a similar magnitude (681 MJ for the non-hierarchical and 683 MJ for the hierarchical variant). The hierarchical MPC can reduce thermal discomfort by 64 % (with 0.72 Kh compared to 1.99 Kh for the non-hierarchical MPC). As exhibited in the ”CCA control input” subplot, the hierarchical variant regulates the CCA in a more dynamic manner, which results in the same Mean Average Error (MAE, 0.001 kg/s; averaged over all rooms) but a higher Root Mean Square Error (RMSE) for the ADMM consensus (0.003 kg/s compared to 0.002 kg/s). The computational time ratio of 0.191 for the hierarchical MPC (computation time of 82 359 s) is approximately 3 times higher than the one of 0.060 for the non-hierarchical MPC (computation time of 25 850 s), which is due to the execution of three lower MPC layer instances during one upper MPC layer MPC operation.

https://doi.org/10.52202/069564-0220

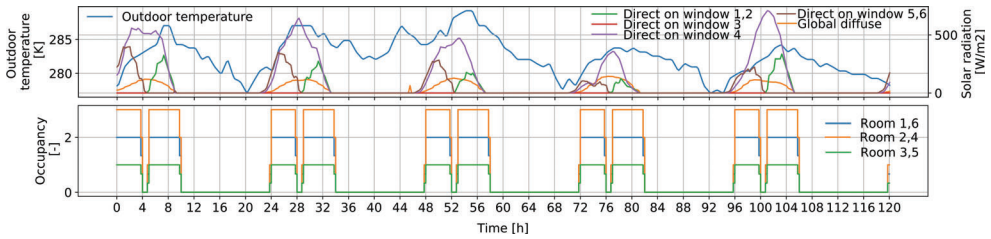

Figure 4: Disturbances for the standard deviations σ = (0,0,0) (perfect forecast)

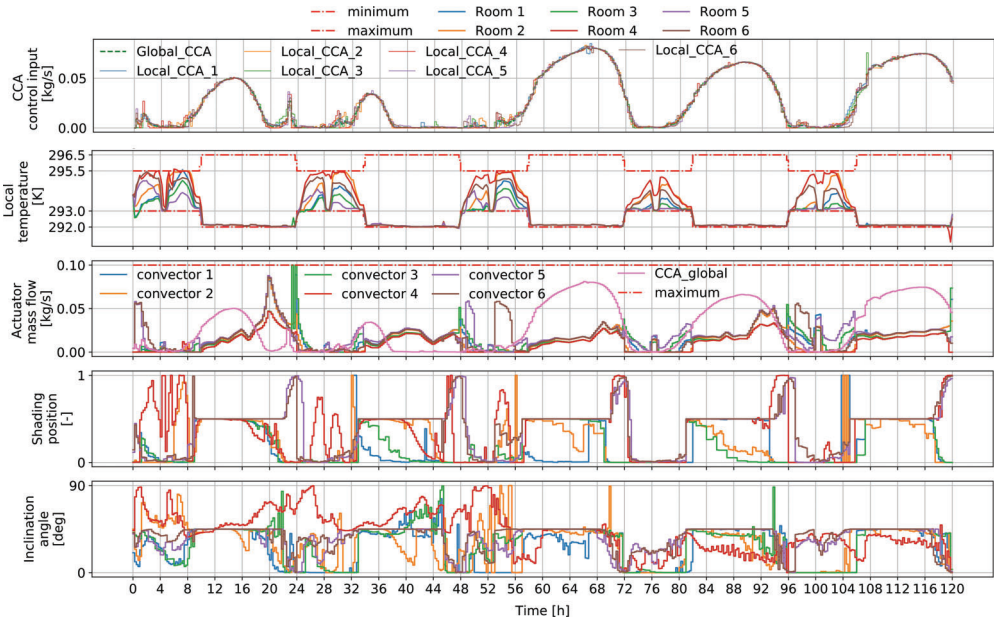

Figure 5: Non-hierarchical distributed MPC for the standard deviations σ = (0,0,0) (perfect forecast)

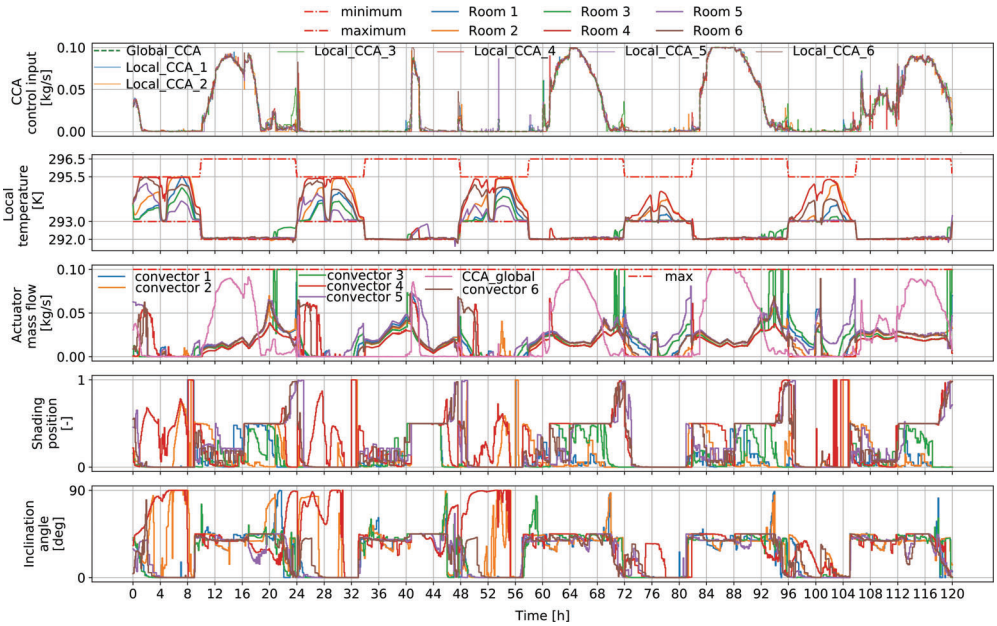

Figure 6: Hierarchical distributed MPC for the standard deviations σ = (0,0,0) (perfect forecast)

Forecast scenario σ = (0.5,50,0.1)

For the second scenario, the forecast errors are artificially generated based on normal distributions with fixed standard deviations for each disturbance quantity (0.5 for occupancy, 50 W/m^2 for the radiation quantities and 0.1 1/h for air exchange). The forecast errors are shown in Fig. 7 and range up to $\pm$1 for occupancy, $\pm$100 W/m^2 for the solar radiation quantities and $\pm$0.2 1/h for air exchange.

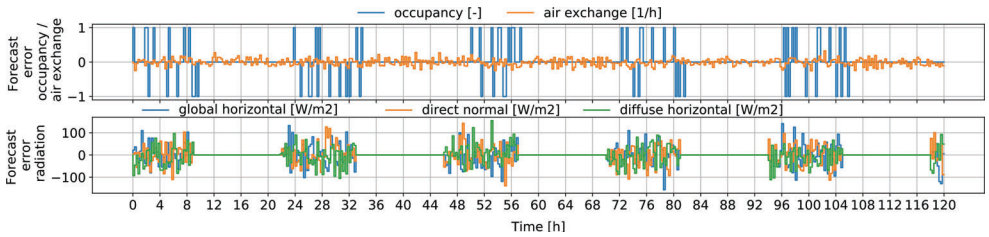

Figure 7: Forecast errors for the standard deviations σ = (0.5,50,0.1)

The simulation results for the non-hierarchical and the hierarchical distributed MPC are visualized in Fig. 8 and Fig. 9. As shown in the "Local temperature" subplots, the hierarchical MPC exhibits an increased reactivity to the occurring forecast errors and a higher capability of preserving thermal comfort and operating the room temperatures between the comfort bounds. For the non-hierarchical MPC, especially the lower comfort bounds are exceeded more frequently. This manifests itself during non-occupancy (e.g., during hours 38–46) and particularly during occupancy periods (e.g., during hours 48–58 and 72-84), when forecast errors are imposed on all disturbance quantities (see Fig. 7). The hierarchical MPC can reduce the thermal discomfort resulting from the operation of the non-hierarchical MPC (24.30 Kh) by 9.62 Kh (equivalent to a reduction of 39.6 %) resulting in a thermal discomfort of 14.68 Kh. The energy consumption for the hierarchical and non-hierarchical MPC are identical (679 MJ). The last three subplots of Fig. 8 and Fig. 9 reveal that the control inputs of the hierarchical MPC are operated in a more dynamic way to compensate for the forecast errors. The "CCA control input" subplots show a similar convergence for both MPC variants with few diverging outliers, which leads to an identical consensus MAE of 0.001 kg/s and an RMSE of 0.002 kg/s. The computation time for the hierarchical MPC (61 691 s) is approximately 3.4 times higher than the one for the non-hierarchical variant (18 173 s). The hierarchical MPC is seven times faster than real-time according to a computational time ratio of 0.14.

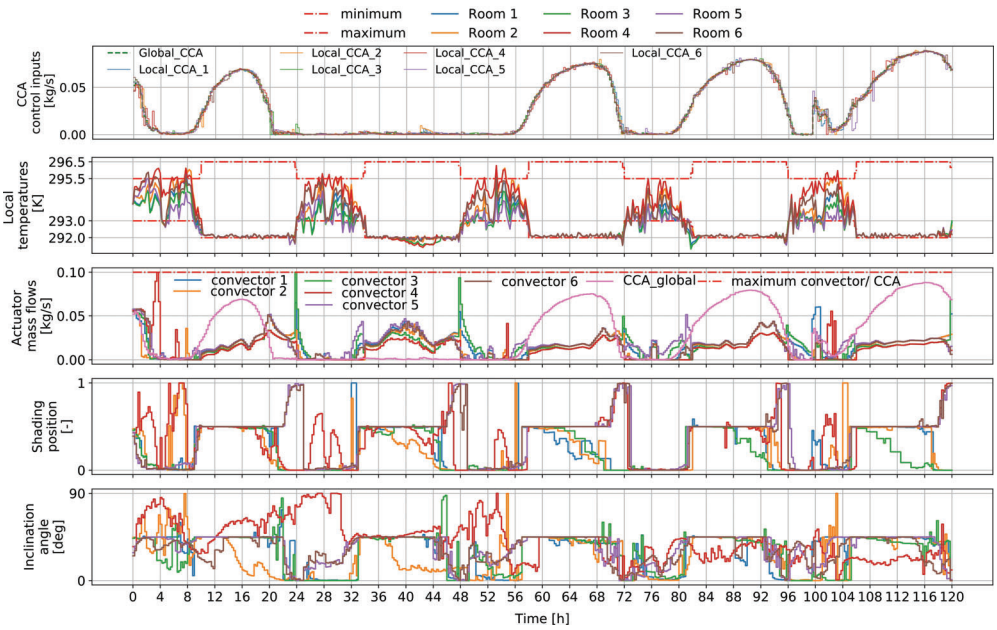

Figure 8: Non-hierarchical distributed MPC for the standard deviations σ = (0.5,50,0.1)

https://doi.org/10.52202/069564-0220

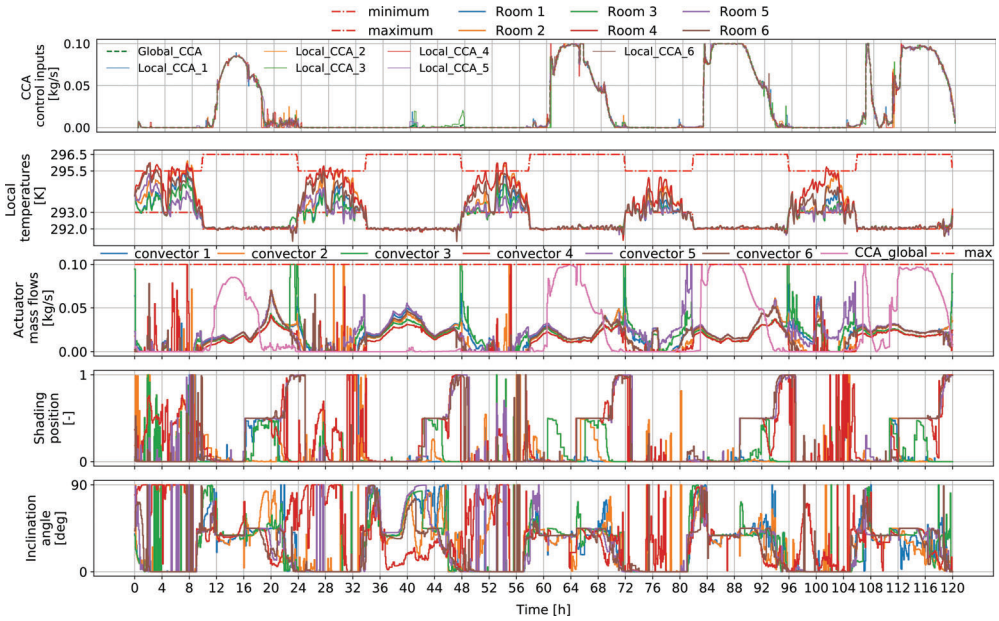

Figure 9: Hierarchical distributed MPC for the standard deviations σ = (0.5,50,0.1)

Forecast scenario σ = (1,100,0.2)

Figure 10 depicts the forecast errors for the σ = (1,100,0.2) scenario, which range up to $\pm$2 for occupancy, $\pm$200 W/m^2 for the solar radiation quantities and $\pm$0.4 1/h for air exchange. In Fig. 11 and Fig. 12, the performance of the non-hierarchical and hierarchical distributed MPC for this forecast scenario are shown. In analogy with the previous forecast scenario, the "Local temperature" subplots manifest a substantially increased reactivity and ability of the hierarchical MPC to compensate for forecast errors. This shows itself by reducing the exceedance of both the lower (e.g., during hours 24–34, 34–48 and 72–82) and upper comfort bounds (e.g., during hours 100–106). The benefits of the hierarchical MPC are particularly revealed complying with the lower comfort bound, since in this case study, only heating actuators are included that are able to react to the forecast errors (apart from the predictive "cooling" function of the solar shading). The exceedance of the comfort bounds, which is attributed to the deviation between predicted and real disturbance quantities, can be compensated in a shorter time by the hierarchical MPC benefiting from the small sampling period of the lower MPC layer. Thermal discomfort can be reduced from 43.25 Kh for the non-hierarchical to 30.91 Kh for the hierarchical MPC, which corresponds to a decrease of 28.5 % or an absolute reduction of 12.34 Kh. Again, the consumed energy is identical for both variants with 678 MJ.

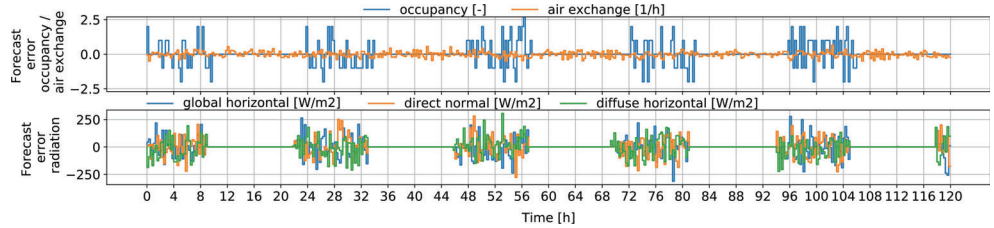

Figure 10: Forecast errors for the standard deviations σ = (1,100,0.2)

The subplots "Actuator mass flow", "Shading position" and "Inclination angle" exhibit the more dynamic operation of the control inputs. The potentially disturbing effect of frequent shading or wear and tear is not considered here. The focus is placed on the reactivity of the control and preservation of comfort. In future versions, constraining or penalizing the change in control inputs between two iterations could be added. The "CCA control input" subplots show a comparable ADMM convergence for both MPC variants with an identical MAE of 0.001 kg/s and a consensus RMSE of 0.002 kg/s. The increased reactivity of the hierarchical MPC comes at the cost of three times larger computation times (computation time of 67 897 s for the hierarchical

and 20 245 s for the non-hierarchical MPC). With a computational time ratio of 0.16, the hierarchical MPC is six times faster than real-time.

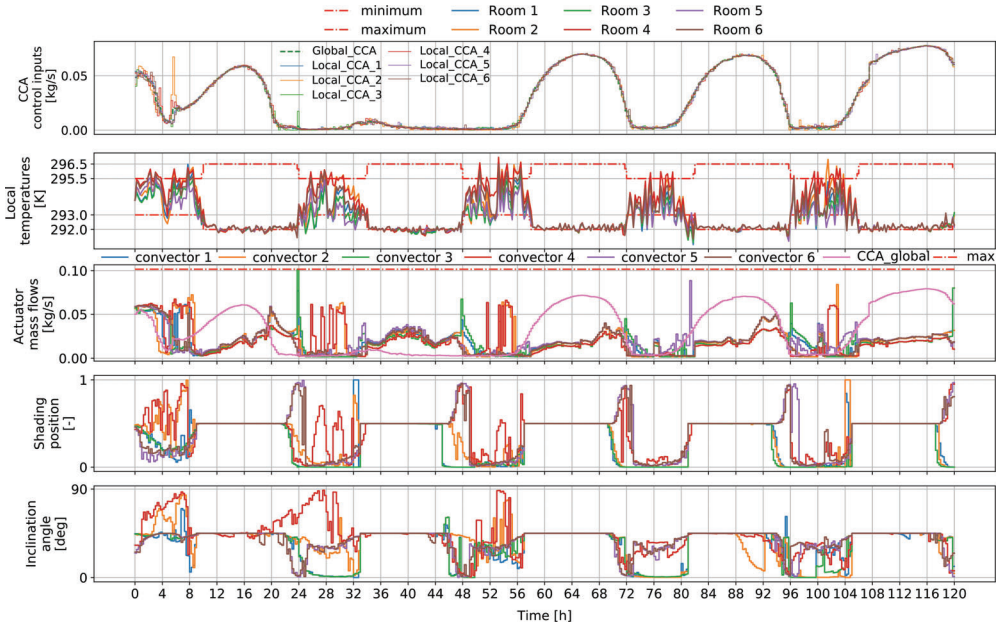

Figure 11: Non-hierarchical distributed MPC for the standard deviations σ = (1,100,0.2)

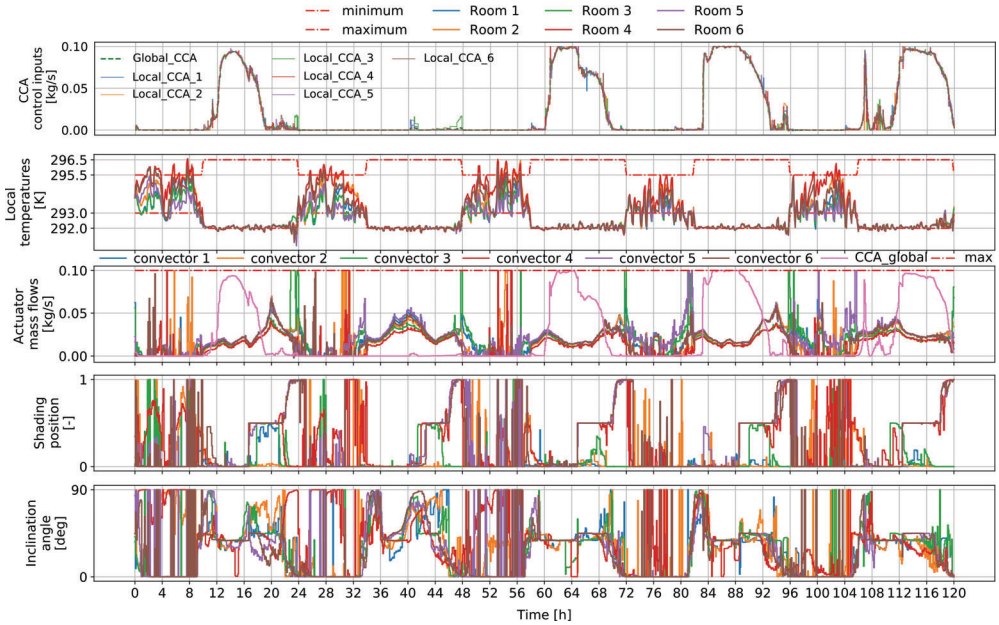

Figure 12: Hierarchical distributed MPC for the standard deviations σ = (1,100,0.2)

5. Conclusion

In this work, a hierarchical distributed MPC for building energy systems based on nonlinear Modelica controller models is presented. The MPC concept couples hierarchical and distributed optimization approaches to divide the optimization complexity within the temporal and spatial dimension and enable decoupled, modular modeling. The hierarchical optimization approach takes into account different dynamics in buildings and guarantees

https://doi.org/10.52202/069564-0220

both anticipation for components with high inertia and time delay as well as reactivity with respect to deviations between the predicted and the actual building behavior. The distributed optimization approach splits the optimization problem into subproblems to improve the scalability and real-time capability of the control while accounting for the coupling between the subproblems.

The flexibility and robustness of the proposed control approach are evaluated for different scenarios of the forecast accuracy for the disturbance quantities of occupancy, solar radiation and air exchange. The artificially generated forecast errors can be considered representative of any deviation between the predicted and real-world behavior of buildings. Applied to a six-room building Modelica model, the hierarchical distributed MPC demonstrates a considerably increased capability to keep the room temperatures within the comfort bounds and a relative discomfort reduction of 29 to 40 % for the scenarios with forecast errors in comparison to a non-hierarchical reference MPC. With an increase in forecast errors, the absolute thermal comfort that can be reduced by the hierarchical MPC increases. The increased reactivity comes at the cost of increased computation times. In the case study, the hierarchical distributed MPC manifests a good ADMM convergence and real-time capability by being six times faster than real-time.

In future work, the developed MPC framework will be practically applied to a multi-zone building including dynamic and inert (heating) actuators. Within the hierarchical MPC configuration, different model approximations/linearizations could be evaluated on the different layers focusing on specific components. Finally, integer optimization variables should be included for wider applicability in building control.

Acknowledgments

We gratefully acknowledge the financial support provided by the BMWK (Federal Ministry for Economic Affairs and Climate Action), promotional reference 03EGB0010A.

References

[1] United Nations Environment Programme. *2021 Global Status Report for Buildings and Construction: Towards a Zero-emission, Efficient and Resilient Buildings and Construction Sector*, 2021. URL `https://globalabc.org/resources/publications/2021-global-status-report-buildings-and-construction`.

[2] International Energy Agency. *Building Energy Performance Metrics- Supporting Energy Efficiency Progress in Major Economies*, 2015. URL `https://www.iea.org/reports/building-energy-performance-metrics`.

[3] Serale, G., Fiorentini, M., Capozzoli, A., Bernardini, D., Bemporad, A. *Model Predictive Control (MPC) for enhancing building and HVAC system energy efficiency: Problem formulation, applications and opportunities*. Energies, 11(3, 631), 2018. doi: 10.3390/en11030631.

[4] Drgoňa, J., Arroyo, J., Cupeiro Figueroa, I., Blum, D., Arendt, K., Kim, D., Ollé, E. P., Oravec, J., Wetter, M., Vrabie, D. L., Helsen, L. *All you need to know about model predictive control for buildings*. Annu. Rev. Control, 50:190–232, 2020. doi: 10.1016/j.arcontrol.2020.09.001.

[5] Cigler, J., Gyalistras, D., Siroky, J., Tiet, V.-N., Ferkl, L. *Beyond Theory: the Challenge of Implementing Model Predictive Control in Buildings*. In 11th REHVA world Congr. 8th Int. Conf. Energy Effic. Smart Heal. Build., pages 1008–1018, 2013.

[6] Mattsson, S. E., Elmqvist, H. *Modelica - An International Effort to Design the Next Generation Modeling Language*. IFAC Proc. Vol., 30(4):151–155, 1997. doi: 10.1016/s1474-6670(17)43628-7.

[7] Wetter, M., Van Treeck, C. *New Generation Computational Tools for Building and Community Energy Systems Annex 60 Final Report*. 2017. URL `http://www.iea-annex60.org/downloads/iea-ebc-annex60-final-report.pdf`.

[8] Scattolini, R. *Architectures for distributed and hierarchical Model Predictive Control – A review*. J. Process Control, 19(5):723–731, 2009. doi: 10.1016/j.jprocont.2009.02.003.

[9] Koehler, S., Danielson, C., Borrelli, F. *A primal-dual active-set method for distributed model predictive control*. Optim. Control Appl. Methods, 38(3):399–419, 2017. doi: 10.1002/oca.2262.

[10] Moroşan, P. D., Bourdais, R., Dumur, D., Buisson, J. *A distributed MPC strategy based on Benders' decomposition applied to multi-source multi-zone temperature regulation*. J. Process Control, 21(5):729–737, 2011. doi: 10.1016/j.jprocont.2010.12.002.

[11] Ma, Y., Anderson, G., Borrelli, F. *A distributed predictive control approach to building temperature regulation*. In Proc. 2011 Am. Control Conf., pages 2089–2094, San Francisco, CA, USA, 2011. IEEE. doi: 10.1109/acc.2011.5991549.

[12] Scherer, H. F., Pasamontes, M., Guzmán, J. L., Álvarez, J. D., Camponogara, E., Normey-Rico, J. E. *Efficient building energy management using distributed model predictive control*. J. Process Control, 24 (6):740–749, 2014. doi: 10.1016/j.jprocont.2013.09.024.

[13] Baranski, M., Fütterer, J., Müller, D. *Distributed exergy-based simulation-assisted control of HVAC supply chains*. Energy Build., 175:131–140, 2018. doi: 10.1016/j.enbuild.2018.07.006.

[14] Moroşan, P. D., Bourdais, R., Dumur, D., Buisson, J. *Distributed model predictive control for building temperature regulation*. In Proc. 2010 Am. Control Conf., pages 3174–3179, Baltimore, MD, USA, 2010. IEEE. doi: 10.1109/acc.2010.5530977.

[15] Li, Z., Zhang, J. *Study on the distributed model predictive control for multi-zone buildings in personalized heating*. Energy Build., 231:110627, 2021. doi: 10.1016/j.enbuild.2020.110627.

[16] Cai, J., Kim, D., Jaramillo, R., Braun, J. E., Hu, J. *A general multi-agent control approach for building energy system optimization*. Energy Build., 127:337–351, 2016. doi: 10.1016/j.enbuild.2016.05.040.

[17] Li, W., Wang, S. *A multi-agent based distributed approach for optimal control of multi-zone ventilation systems considering indoor air quality and energy use*. Appl. Energy, 275:115371, 2020. doi: 10.1016/j.apenergy.2020.115371.

[18] Hou, X., Xiao, Y., Cai, J., Hu, J., Braun, J. E. *Distributed model predictive control via Proximal Jacobian ADMM for building control applications*. In Proc. Am. Control Conf., pages 37–43, Seattle, WA, USA, 2017. IEEE. doi: 10.23919/ACC.2017.7962927.

[19] Lin, F., Adetola, V. *Flexibility characterization of multi-zone buildings via distributed optimization*. In 2018 Annu. Am. Control Conf., pages 5412–5417, Milwaukee, WI, USA, 2018. IEEE. doi: 10.23919/ACC.2018.8431400.

[20] Abreu, A., Bourdais, R., Guéguen, H. *Inter-Layer Interactions in Hierarchical MPC for Building Energy Management Systems*. IFAC-PapersOnLine, 50(1):12027–12032, 2017. doi: 10.1016/j.ifacol.2017.08.2136.

[21] Fiorentini, M., Cooper, P., Ma, Z., Robinson, D. A. *Hybrid Model Predictive Control of a Residential HVAC System with PVT Energy Generation and PCM Thermal Storage*. Energy Procedia, 83:21–30, 2015. doi: 10.1016/j.egypro.2015.12.192.

[22] Long, Y., Liu, S., Xie, L., K. H., J. *A hierarchical distributed MPC for HVAC systems*. In 2016 Am. Control Conf., pages 2385–2390, Boston, MA, USA, 2016. IEEE. doi: 10.1109/ACC.2016.7525274.

[23] Mork, M., Xhonneux, A., Müller, D. *Hierarchical Model Predictive Control for complex building energy systems*. Bauphysik, 42(6):306–314, 2020. doi: 10.1002/bapi.202000031.

[24] Mork, M., Xhonneux, A., Müller, D. *Nonlinear Distributed Model Predictive Control for multi-zone building energy systems*. Energy Build., 264:112066, 2022. doi: 10.1016/j.enbuild.2022.112066.

[25] Boydens, W., Helsen, L., Olesen, B. W., Laverge, J. *Renewable and Storage-integrated Systems to Supply Comfort in Buildings*. A & S/books on Architecture and Arts, 2021. doi: 10.5281/zenodo.5109932.

[26] Boyd, S., Parikh, N., Chu, E., Peleato, B., Eckstein, J. *Distributed optimization and statistical learning via the alternating direction method of multipliers*. Found. Trends Mach. Learn., 3(1):1–122, 2010. doi: 10.1561/2200000016.

[27] Müller, D., Lauster, M., Constantin, A., Fuchs, M., Remmen, P. *Aixlib - an Open-Source Modelica Library Within the IEA-EBC Annex 60 Framework*. In Proc. CESBP Cent. Eur. Symp. Build. Phys. BauSIM 2016, pages 3–9, Dresden, Germany, 2016.

[28] Åkesson, J., Årzén, K. E., Gäfvert, M., Bergdahl, T., Tummescheit, H. *Modeling and optimization with Optimica and JModelica.org-Languages and tools for solving large-scale dynamic optimization problems*. Comput. Chem. Eng., 34(11):1737–1749, 2010. doi: 10.1016/j.compchemeng.2009.11.011.

[29] *HSL. A collection of Fortran codes for large scale scientific computation.*, 2013. URL `http://www.hsl.rl.ac.uk/`.

[30] Wächter, A., Biegler, L. T. *On the implementation of an interior-point filter line-search algorithm for large-scale nonlinear programming*. Math. Program., 106(1):25–57, 2006. doi: 10.1007/s10107-004-0559-y.

https://doi.org/10.52202/069564-0220